01 Feb 2008

A Suite of Robust Controllers for the Manipulation of Microscale Objects

Qinmin Yang

Jagannathan Sarangapani
Missouri University of Science and Technology, sarangap@mst.edu

Recommended Citation

Q. Yang and J. Sarangapani, "A Suite of Robust Controllers for the Manipulation of Microscale Objects," *IEEE Transactions on Systems, Man and Cybernetics*, Institute of Electrical and Electronics Engineers (IEEE), Feb 2008.
The definitive version is available at https://doi.org/10.1109/TSMCB.2007.909943

A Suite of Robust Controllers for the Manipulation of Microscale Objects

Qinmin Yang, *Student Member, IEEE*, and S. Jagannathan, *Senior Member, IEEE*

***Abstract*—A suite of novel robust controllers is introduced for the pickup operation of microscale objects in a microelectromechanical system (MEMS). In MEMS, adhesive, surface tension, friction, and van der Waals forces are dominant. Moreover, these forces are typically unknown. The proposed robust controller overcomes the unknown contact dynamics and ensures its performance in the presence of actuator constraints by assuming that the upper bounds on these forces are known. On the other hand, for the robust adaptive critic-based neural network (NN) controller, the unknown dynamic forces are estimated online. It consists of an action NN for compensating the unknown system dynamics and a critic NN for approximating a certain strategic utility function and tuning the action NN weights. By using the Lyapunov approach, the uniform ultimate boundedness of the closed-loop manipulation error is shown for all the controllers for the pickup task. To imitate a practical system, a few system states are considered to be unavailable due to the presence of measurement noise. An output feedback version of the adaptive NN controller is proposed by exploiting the separation principle through a high-gain observer design. The problem of measurement noise is also overcome by constructing a reference system. Simulation results are presented and compared to substantiate the theoretical conclusions.**

***Index Terms*—Adaptive neural network (ANN), micromanipulation, reinforcement learning, robust controller.**

I. Introduction

MICROELECTROMECHANICAL systems (MEMS) are a relatively new technology involving the miniaturization of systems areand components to create complex machines that are of micrometer size in nature. These are used in a variety of applications involving sensing, actuation, and communication. The MEMS has revolutionized a major part of the sensor and actuator industry. Typical MEMS products include inkjet printer heads and accelerometers for airbags [1]. Although these products require little or no assembly, automatic assembly of hybrid MEMS devices is desirable. Much effort has been put forth for the microassembly or micromanipulation [1], [2], [4]–[6], [11]–[14]. Among them, in [1], the pickup and release tasks with van der Waals force are analyzed, whereas in [6], manipulation using a scanning electron microscope (SEM) is introduced. Research effort in [4] proposed a manipulation system in open air and fulfilled manipulations with a gold-coated piezoresistive silicon cantilever.

Modeling of such microscale devices for actuation is a whole lot different than in macroscale system. At microscale, surface forces are predominant, whereas volumnic forces are negligible [1]. The dominant forces acting on a MEMS system are mainly van der Waals, capillary, and electrostatic forces, whereas the forces due to gravity are negligible. Typically, these forces vary much with environment and could not be precisely measured. Furthermore, uncertainties, for instance, fabrication imperfections and complex system nonlinearities, make the actuation and manipulation of such devices difficult.

At the same time, modeling and simulation are critical and fundamental for designing proper handling techniques. Work on the modeling adhesive forces and the utilization of the models in micromanipulation have been carried out by many researchers. Arai *et al.* [5] studied the effects of attractive forces and handling strategies in micromanipulation. Rollot *et al.* [28] studied various modes in micromanipulation by combining analytical microforce models and Newton–Euler dynamics, whereas Sitti and Hashimoto [29] built the model for manipulation of nanoparticles, and Feddema *et al.* [30] introduced a computational model of van der Waals forces and electrostatic forces for interactions between a microsphere and a microcube.

Designing controllers for the manipulation and handling of microscale objects poses a much greater challenge in terms of accommodating the nonlinearities in the system. Hence, these forces have to be modeled to design a controller for the MEMS. To confront some of the issues of nonlinearities and uncertainties in such MEMS, a robust controller is designed. The robust controller requires the upper bound on the uncertainties and nonlinearities.

Moreover, in practical control problems, the amplitude of the control signal is subject to prescribed actuator constraints due to saturation. Ignoring these constraints may lead to unsatisfactory performance or even instability of the closed-loop system. In adaptive control systems, the saturation problem becomes particularly critical because of the parameter adaptation transients, which may introduce large control signals [25]. However, the research activity devoted to the problem of controlling a nonlinear system in the presence of saturation is still limited [23], [24]. Thus, in this paper, actuator constraints have been incorporated into the robust controller design, in contrast to other works [7], where no explicit magnitude constraints are treated.

On the other hand, in the case of a robust adaptive critic-based neural network (NN) controller, the reinforcement

Manuscript received November 10, 2006; revised August 27, 2007 and September 10, 2007. This work was supported in part by ECCS 0216191, by ECS 0621924, and by the Intelligent Systems Center. This paper was recommended by Associate Editor F. L. Lewis.

The authors are with the Department of Electrical and Computer Engineering, University of Missouri-Rolla, Rolla, MO 65401 USA (e-mail: qyy74@umr.edu).

Color versions of one or more of the figures in this paper are available online at http://ieeexplore.ieee.org.

Digital Object Identifier 10.1109/TSMCB.2007.909943

learning feature [11] is utilized to approximate the uncertainties online. The reinforcement-learning-based NN (RLNN) structure consists of two NNs: 1) an action NN for compensating the uncertain nonlinear system dynamics and 2) a critic NN for tuning the weights of the action NN. A novel utility function, which is viewed as the system performance index over time, was defined as the critic NN input. The critic signal approximates the long-term performance measure and provides an additional corrective action based on current and past long-term system performance, in contrast with the standard adaptive dynamic programming scheme [9], [16]–[18], where the critic signal alone is used to tune the action NN weights, and in standard adaptive NN (ANN) control literature, where a short-term performance is normally utilized [7]. The critic NN output along with the filtered tracking error is used to tune the action NN.

Providing tracking error information to the action NN will make the proposed controller similar to the other adaptive controllers [7]; therefore, it is avoided. Moreover, a Lyapunov approach is used to show the stability of the closed-loop system in contrast with the existing schemes in adaptive dynamic-programming-based critic NN control schemes [16]–[18]. The proposed NN structure has an advantage over supervised learning NN-based controllers, where the desired system outputs are not required. In our scenario, the desired outputs are the probe location and the contact dynamics, which are typically unknown. An offline learning phase is not required in this approach, in contrast with adaptive dynamic-programming-based critic control schemes [16]–[18].

Finally, in many practical problems, not all state variables are measurable due to technical or economic reasons [33]. For instance, in the micromanipulation system, a laser measuring instrument [32] or a SEM [13] is employed to obtain the position of the microobjects, whereas the velocities are not measured. Nevertheless, the obtained information is usually contaminated with measurement noise. Therefore, an output feedback controller is designed by implementing a high-gain observer, which is used to estimate the actual system states, which also include the velocities. The bounded measurement noise is integrated into a new reference system and overcome. Theoretical and simulation results indicate that the output feedback ANN controller is able to successfully perform the task.

Therefore, in this paper, both robust and adaptive critic-based NN controllers, and their output feedback version are proposed for the pickup task in a micromanipulation system. These two controllers are contrasted based on their performance. The main contributions of this paper can be summarized as follows.

1) A computation model for the pickup task is formulated, considering the unknown microadhesive forces including van der Waals, surface tension, and electrostatic forces.
2) A robust controller is designed to accommodate the unknown interactive microforces for the task of picking up the microparticles.
3) An adaptive critic-based NN scheme is introduced to achieve a better response—a cost function is utilized to evaluate the system performance. The NNs are updated in an online fashion without offline training phase, and the persistent excitation condition requirement is overcome.
4) To overcome the unmeasured states in the presence of measurement noise, a high-gain observer is added with the NN controller.

A brief background on NNs and the stability of the nonlinear system are given in Section II. The interactive force analysis of the pickup task and associated dynamic models are presented in Sections III and IV, respectively. Next, the robust and ANN controller designs are given in Section V. Finally, Section VI shows the simulation results to substantiate our theoretical conclusions.

II. Background

A. NN Background

A general function $f(x) = C^{(s)}$ can be approximated using an NN with, at least, two layers of appropriated weights given by

$$f(x) = W^T \sigma(V^T x) + \zeta \tag{1}$$

where W and V are constant-weight matrices of the NN (the first column of these matrices include the bias vectors, so that tuning the weight matrices results in tuning the biases as well), x is the input vector, $\sigma(V^T x)$ is the vector of the hidden-layer activation functions, and ζ is the error in approximation. If the input to the hidden-layer weight matrix V is selected randomly and kept constant, and the vector of the hidden-layer activation functions is selected as a basis function, whereas the output layer weights are only tuned, provided that a sufficiently large number of nodes in the hidden layer are chosen, then a one-layer NN will result [10]. For simplicity, define the net output for a one-layer NN as

$$y = W^T \sigma(x) + \zeta. \tag{2}$$

For suitable approximation, $\sigma(x)$ must form a basis to the function that is being approximated. Since it is already known that (2) can approximate any continuous function over a compact set and a set of target weights exists, then the control objective is to tune the weights such that they approach their target values.

NN controller designs have relied on the function approximation property (1) [15]. Thus, the performance of the controller mainly depends on the learning algorithm, as suggested in [16]. Among various NN controller structures, adaptive critic designs [16] utilize reinforcement learning for NN weight tuning. These designs address the general problem of how to optimize a measure of utility or goal function in an unknown, noisy, and nonlinear system.

In a typical adaptive critic NN architecture, the critic NN evaluates the system performance index and tunes the action generating NN, which in turn provides the control input signal to the plant to be controlled. Many papers that deal with control using the adaptive critic NN architecture are mentioned here. For details, see [9] and [16]–[18]. However, very few papers [16] present the closed-loop stability analysis with performance guarantee. This paper overcomes these limitations by using the

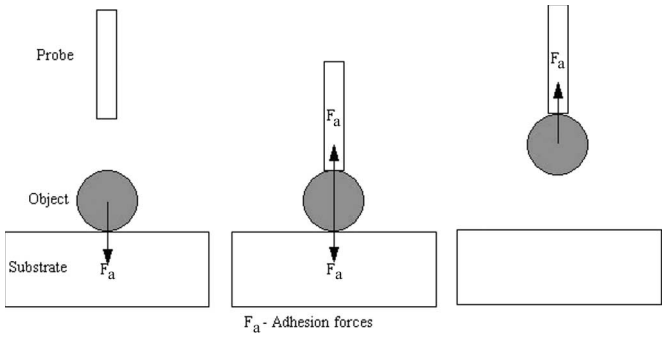

Fig. 1. Object-handling task.

Lyapunov approach for control applications. Next, the following definition is required.

B. Stability of Closed-Loop Systems

Consider a nonlinear system given by

$$\dot{x} = f(x, u)$$
$$y = h(x) \tag{3}$$

where x is the state vector, u is the input vector, and y is the output vector [6]. For a control input u, the closed-loop system (3) is uniformly ultimately bounded (UUB), if for all $x(t_0) = x_0$, there exist a $\varepsilon > 0$ and a constant $T = T(x_0, \varepsilon)$, such that $\|x(t)\| < \varepsilon$ for all $t \geq t_0 + T$.

III. Interaction Force Model

Manipulation and handling of microscale objects are required for the assembly and maintenance of micromachines and their parts. In this paper, we consider the manipulation of microsized sphere-shaped objects or microparticles that are 50 μm in diameter. When manipulating objects in the microdomain, the pickup should be understood using microphysics [2], [3]. Modeling is necessary for picking up and placing microspheres laying on a planar substrate. In the manipulation process, the microsphere is to be picked up and placed at another location for assembly. As a brief description, the probe, which is treated as the end effector and manipulator, is lowered to make contact with the microsphere. Once contact has been established, the microobject has to be picked up by retracting the probe as a result of adhesive forces [4]. Next, the probe will be moved with the microobjects to a desired target position. After that, the object will be placed on the substrate by creating a repulsive force.

However, the process of placing the microobject is also an intricate process and different from that of the pickup. Generally, by selecting proper system parameters, the spheres can be picked up by the probe due to the attractive force between them [1]. On the other hand, the job of releasing the spheres needs totally different techniques. Various placing methods have been introduced in [1], [13], [14], and [31]. For instance, in [31], electrostatic interaction is utilized. In this paper, we will concentrate our work on the pickup task of microspheres.

For the purpose of designing a controller for the object-handling task, we shall restrict ourselves with the intricacies of the physics during the pickup process, as shown in Fig. 1.

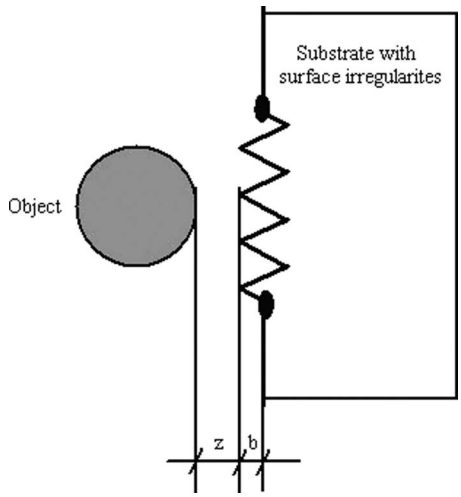

Fig. 2. Rough plate and plane sphere.

The adhesion forces are dominant in the system. They are considered to play an important role in the manipulation process. These are given by the following:

- van der Waals forces;
- surface tension (or capillary);
- electrostatic (or Coulomb) forces.

A. Van der Waals Force

The van der Waals force acts between atoms resulting from the interaction between electrons in the outermost bands rotating around the nucleus of the atoms. An overview of it is given in [19]. Van der Waals forces are present in every environmental condition. Depending on the object geometry and material type, the van der Waals force can be calculated based on the interaction energy between atoms or molecules. For ideal geometries, the van der Waals forces are given by

$$F_{\rm bp}^{\rm VdW} = \frac{A_{\rm bp}^{w} R_b}{6 D_{\rm bp}^2}$$
$$F_{\rm bs}^{\rm VdW} = \frac{A_{\rm bs}^{w} R_b}{6 D_{\rm bs}^2}$$
$$F_{\rm bb}^{\rm VdW} = \frac{A_{\rm bb}^{w} R_b}{6 D_{\rm bb}^2} \tag{4}$$

for ball–probe (bp), ball–substrate (bs), and ball–ball interactions, respectively. Here, R_b is the sphere radius, A_{ij}^{w} is the Hamaker constant of the "$i-$water$-j$" interface, and D_{ij} is the separation distance. Furthermore, van der Waals forces are greatly influenced by the surface roughness [2]. It has been shown that increasing the surface roughness decreases the van der Waals forces [4]. Thus, taking the surface roughness into consideration, as shown in Fig. 2, the van der Waals force is expressed as [6]

$$F_{\rm vdwb} = \left(\frac{z}{z + b/2} \right)^2 F_{\rm vdw} \tag{5}$$

where z is the distance, b is the height of the surface irregularities, and $F_{\rm vdw}$ is the van der Waals forces between the plane plate and the sphere.

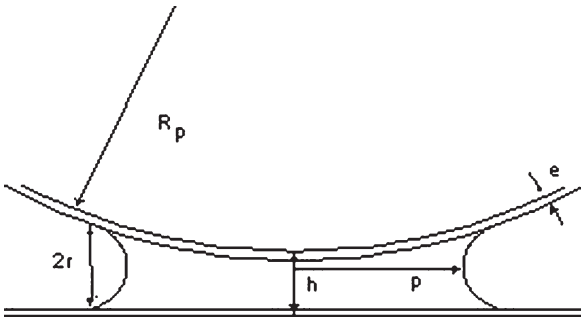

Fig. 3. Capillary force parameters during a sphere and flat surface contact.

B. Surface Tension Force

In ambient operational environment, the water layer is present on the surface of the sphere and the substrate. A liquid bridge occurs between them at close contact, as shown in Fig. 3.

In [20], the macroscopic theory of capillarity is proven to be applicable for a curvature radius on the order of molecular size. Assuming that 1) $r \ll p \ll R_p$; 2) the surfaces are coated with a film of constant thickness e; 3) the contact angle is 0, which should be the true in our case; and 4) the surface attraction through the liquid phase is negligible, the capillary force can be written as [21]

$$F^{\text{cap}} = 4\pi\gamma R_p \left(1 - \frac{h-2e}{2r}\right) \tag{6}$$

where γ is the liquid (water) surface energy, e is the thickness of the water layer, and r is the radius of curvature of the meniscus, as shown in Fig. 3. Moreover, the volume of liquid condensed in the bridge and the film thickness distribution can also influence the capillary force, but it can be ignored in our case [21]. The capillary forces for the bp and bs interactions can be calculated from (6). It is important to notice that baking the sample before the manipulation process can greatly reduce the capillary forces [21].

C. Electrostatic Force

For the electrostatic force, Coulomb forces are considered only. Using the point charge Assumption, the electrostatic force between an uncharged metal wall and a charged sphere is given by

$$F^{\text{elec}} = \varepsilon_0 \pi d^2 \left(\frac{3\varepsilon_1}{\varepsilon_1 + 2}\right)^2 E^2 \tag{7}$$

where ε_0 and ε_1 are the dielectric constants of free space and the material, respectively. Parameter d is the diameter obtained as $d = d_1 d_2 / d_1 + d_2$, where d_1 and d_2 are the diameters of the two microspheres under consideration. Parameter E is the voltage between the probe and the substrate. It has also been shown that the electrostatic forces can be minimized by applying an external voltage.

IV. Dynamic Model

A dynamic model of the microscale-object-handling system is formulated, considering all the aforementioned forces [4],

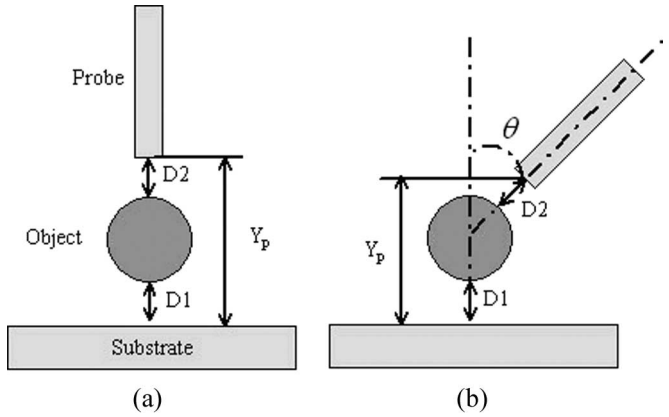

Fig. 4. Intersurface distance notation. (a) Capture at a flat surface and (b) capture at an inclination.

[7]. The objects considered in this paper include microspheres with a diameter in the range of 50–200 μm (radius R_b varies from 25 to 100 μm). In particular, we will also assume a rectangular-block-shaped probe.

When the system is shown as Fig. 4, the dynamic model for the object-handling task can be written as [4]

$$\begin{aligned} m_p \ddot{Y}_p = {} & F_{\text{ext}} \sin(\pi/2 - \theta) - F_{\text{bp}}^{\text{VdW}} \cos\theta \\ & - F_{\text{bp}}^{\text{cap}} \cos\theta - F_{\text{bp}}^{\text{elec}} \cos\theta - m_p g \end{aligned} \tag{8}$$

$$\begin{aligned} m_b \ddot{D}_1 = {} & \left(F_{\text{bp}}^{\text{VdW}} + F_{\text{bp}}^{\text{cap}} + F_{\text{bp}}^{\text{elec}}\right) \cos\theta \\ & - F_{\text{bs}}^{\text{VdW}} - F_{\text{bs}}^{\text{cap}} - F_{\text{bs}}^{\text{elec}} - m_b g \end{aligned} \tag{9}$$

$$Y_p = D_1 + R_b + (R_b + D_2)\cos\theta \tag{10}$$

where $\ddot{Y}_p$ is the instantaneous acceleration of the probe, F_{ext} is the external force applied on the probe, θ is the angle of inclination of the probe with the vertical axis, F_{ij}^{VdW} is the van der Waals forces, F_{ij}^{cap} is the capillary forces, and F_{ij}^{elec} is the electrostatic forces for the bp and bs interfaces presented in (4)–(7), respectively. Here, m_p is the mass of the probe, and m_b denotes the mass of the microsphere. Thus, D_1 and D_2 can be seen as the system states, whereas F_{ext} is the control input. There are two constraints for this model [22].

1) A condition imposed by the substrate reaction when the ball is in contact with the substrate at $D_1 = D_0 = 0.4$ nm. For capture, it is sufficient to show that $D_2 = D_0$ since D_0 is the atomic contact distance given by 0.4 nm [35], i.e.,

$$D_1 = 0.4 \text{ nm} \Rightarrow \ddot{D}_1 \geq 0. \tag{11}$$

2) A detachment constraint expressed by

$$F_{\text{ext}} > 2R_b \pi W_{\text{ball-water-substrate}} \tag{12}$$

where $W_{\text{ball-water-substrate}}$ is the surface work of adhesion.

Practically, the manipulation time has to be small. Furthermore, the applied force has to be appropriate to prevent ball or substrate deformation. The object and the substrate are

sometimes fragile and will be damaged under improper applied force due to controller design.

From (8)–(10), we can find that the dynamic model for the manipulation and handling of microscale objects are quite nonlinear and unknown. For instance, the water surface energy, thickness of the water layer, Hamaker constant, electric charge density, diameter of the object, height of immersion, and many others are typically unknown. Under these circumstances, one has to apply advanced control schemes in order to manipulate such microscale objects. The control scheme must guarantee object manipulation in the event of such unknown uncertainties without damaging samples.

V. Controller Design

The suite of controller designs proposed in this paper is based on the filtered tracking error formulation [7]. In this paper, by using the filtered tracking error system formulation, the robust and robust adaptive ANN controllers have been given in detail. For the purpose of controller design, θ is considered to be zero, which is a valid approach to pick up microparticles [4], [26]. A similar analysis could be performed for different values of θ as well.

A. Filtered Tracking Error Dynamics Formulation

As previously stated, placing the objects on a substrate requires other intricate processes and will not be discussed in this paper. The pickup of the sphere can be viewed with increased D_1 while making $D_2 = D_0$ (atomic contact distance) when the probe is retracting. For detailed illustration, initially, the sphere is resting on the surface of the substrate, and the probe is parked exactly above the sphere. After the force is applied on the probe, it will move downward and make contact with the sphere. Due to the presence of adhesive forces between the probe and sphere, the microobject will be picked up when the probe is retracted. To accomplish this task, a fundamental condition to be fulfilled [1] will be

$$F_{\rm bp} > F_{\rm bs} + F_g \tag{13}$$

which means that the adhesive force between the ball and probe $F_{\rm bp}$ should be greater than the force of surface attraction $F_{\rm bs}$ plus the gravitational force F_g. This condition is critical for material selection.

Hence, for microobject pickup, the control objective is suitably chosen, as previously mentioned. Differentiating (10) yields

$$\dot{Y}_p = \dot{D}_1 + \dot{D}_2 \tag{14}$$

$$\ddot{Y}_p = \ddot{D}_1 + \ddot{D}_2 \tag{15}$$

$$\ddot{D}_2 = \ddot{Y}_p - \ddot{D}_1. \tag{16}$$

Let the error between the desired and the target position be defined as

$$e = D_2 - D_0. \tag{17}$$

Then, when the error becomes zero, $D_2 = D_0$. If D_1 keeps increasing, this implies that the probe has picked up the microsphere. Differentiating (17) yields

$$\dot{e} = \dot{D}_2 \tag{18}$$

and, furthermore,

$$\ddot{e} = \ddot{D}_2 = \ddot{Y}_p - \ddot{D}_1. \tag{19}$$

Let r be the filtered tracking error, which is defined as

$$r = \dot{e} + \Lambda e \tag{20}$$

where $\Lambda \in R$ is a positive design parameter. Furthermore, differentiating (20) yields

$$\dot{r} = \ddot{e} + \Lambda \dot{e}. \tag{21}$$

Substituting the $\ddot{e}$ and $\dot{e}$ from (18) and (19) results in

$$\dot{r} = \ddot{Y}_p - \ddot{D}_1 + \Lambda \dot{D}_2 = (F_1(Y_p) - F_2(D_1)) + \Lambda \dot{D}_2 + v \tag{22}$$

where

$$F_1(Y_p) = \frac{1}{m_p}\left(-F_{\rm bp}^{\rm VdW} - F_{\rm bp}^{\rm cap} - F_{\rm bp}^{\rm elec} - m_p g\right) \tag{23}$$

$$F_2(D_1) = \frac{1}{m_b}\left(F_{\rm bp}^{\rm VdW} + F_{\rm bp}^{\rm cap} + F_{\rm bp}^{\rm elec}\right) - \frac{1}{m_b}\left(F_{\rm bs}^{\rm VdW} + F_{\rm bs}^{\rm cap} + F_{\rm bs}^{\rm elec} + m_b g\right) \tag{24}$$

and v is the control input given by

$$v = \frac{1}{m_p} F_{\rm ext}. \tag{25}$$

Thus, the tracking error dynamics can be rewritten as

$$\dot{r} = F(X) + \Lambda \dot{D}_2 + v \tag{26}$$

where $F(X) = F_1(Y_p) - F_2(D_1)$ is an unknown nonlinear function, and $X = [Y_p, D_2]^T \in R^2$.

B. Robust Controller Design

Robust controllers have been widely implemented in dynamic systems with unknown or slowly varying uncertain parameters. In our system, a typical robust saturation controller can be selected as

$$\tau = -\hat{F}(X) - \Lambda \dot{D}_2 - k_v r - v_1 \tag{27}$$

where $k_v \in R$ is the feedback gain, and the auxiliary feedback signal v_1 is chosen later, with $\hat{F}(X)$ being an estimate for $F(X)$ that is not updated online.

Assumption 1: Let $F_M(X)$ is a known scalar function that bounds the uncertainties $\tilde{F}(X) = F(X) - \hat{F}(X)$, so that

$$\left\|\tilde{F}(X)\right\| \le F_M(X). \tag{28}$$

The intent is that $F_M(X)$ is a simplified function that can be computed using the bounding properties of the forces that act upon the microsphere. The assumption is standard in robust control literature, such as sliding mode and others [7], [33]. Observing the microforces in Section III, it can be seen that the forces are upper bounded.

Regardless of the saturation constraint, let $v = \tau$, and apply (27) in (26) to obtain

$$\dot{r} = -k_v r + \left(F(X) - \hat{F}(X)\right) + v_1 \tag{29}$$

$$\dot{r} = -k_v r + \tilde{F}(X) + v_1 \tag{30}$$

where $\hat{F}(X)$ is an accurate estimate of $F(X)$; in the presence of no auxiliary signal, then $\tilde{F}(X) \to 0$, and (30) becomes

$$\dot{r} = -k_v r. \tag{31}$$

If k_v is properly selected as a positive constant, then, from (21) and (31), one can readily see that $e \to 0$, with $t \to \infty$. Thus, $D_2 = D_0$, and the sphere is said to be manipulated (pickup task).

However, MEMS and other typical actuators have magnitude constraints, and as a result, the closed-loop stability analysis is more involved since the magnitude constraints of the actuator are treated as saturation nonlinearity. Assuming that $v_{\max}$ is the upper limit for the actuator in order to incorporate the magnitude constraints with the controller, now select the control input as

$$v = \begin{cases} \tau(t), & \text{if } |\tau(t)| \le v_{\max} \\ v_{\max}\text{sgn}\left(\tau(t)\right), & \text{if } |\tau(t)| > v_{\max} \end{cases} \tag{32}$$

where v is the actual control input, and τ is the desired applied force, which is selected to be equal to (27). Hence, we define $\Delta u = v - \tau$ or $v = \tau + \Delta u$. Using (32) in (26) now results in $\dot{r} = -k_v r + \tilde{F}(X) + v_1 + \Delta u$, where Δu can be regarded as a disturbance. In order to combat the disturbance, define $\dot{e}_\Delta$ as

$$\dot{e}_\Delta = -k_v e_\Delta + \Delta u. \tag{33}$$

Now, define the error as

$$e_u = r - e_\Delta. \tag{34}$$

Differentiating (34) and substituting (33) in (34) yield

$$\dot{e}_u(t) = -k_v e_u(t) + \tilde{F}(X) + v_1. \tag{35}$$

Select the auxiliary input in (27) as [7]

$$v_1 = \begin{cases} -e_u \frac{F_M(X)}{|e_u|}, & \text{if } |\tau(t)| \le v_{\max} |e_u| \ge \beta \\ -e_u \frac{F_M(X)}{\beta}, & \text{if } |\tau(t)| \le v_{\max} |e_u| < \beta \\ 0, & \text{if } |\tau(t)| > v_{\max}. \end{cases} \tag{36}$$

In computing the robust control term v_1, β is chosen as a small design parameter.

Theorem 1: Consider the system given in (8)–(10), and take Assumption 1. Then, using the robust controller (32), the errors $|e_u|$, $|r|$, and $|e|$ are eventually bounded to the neighborhood of β.

Proof: We will take the case when $|\tau(t)| \le v_{\max}$. Select the Lyapunov function candidate

$$L = \frac{1}{2} e_u^2. \tag{37}$$

Differentiate the preceding equation and substitute error dynamics (35) to obtain

$$\begin{aligned} \dot{L} &= -k_v e_u^2 + e_u \tilde{F}(X) + e_u v_1 \\ &\le -k_v e_u^2 + |e_u| F_M(X) + e_u v_1. \end{aligned} \tag{38}$$

There are now two cases to consider: $|e_u| \ge \beta$ and $|e_u| < \beta$.

Case 1: $|e_u| \ge \beta$*:* In this case, according to the definition of the robust control term (36), one has

$$\begin{aligned} \dot{L} &\le -k_v e_u^2 + |e_u| F_M(X) - e_u^2 F_M(X)/|e_u| \\ &\le -k_v e_u^2. \end{aligned} \tag{39}$$

Therefore, $\dot{L}$ is negative in terms of $|e_u|$. Hence, L decreases in this region, and $|e_u|$ decreases toward β.

Case 2: $|e_u| < \beta$*:* In this case, according to the definition of the robust control term (36), one has

$$\begin{aligned} \dot{L} &\le -k_v e_u^2 + |e_u| F_M(X) - e_u^2 F_M(X)/\beta \\ &\le -k_v e_u^2 + |e_u| F_M(X) \left(1 - |e_u|/\beta\right). \end{aligned} \tag{40}$$

The last term is generally positive in this region, so nothing can be said about whether L is increasing or decreasing. In general, L may be increasing in this region, so that $|e_u|$ increases toward β. Given the boundedness of $|e_u|$ and using (34), one can conclude that $|r|$ is bounded. Using (20), $|e|$ is bounded.

Similarly, the proof can be shown when $|\tau(t)| > v_{\max}$.

C. ANN Controller Design

In the preceding section, a robust controller with input magnitude constraints is presented wherein the unknown dynamics of the manipulation system is overcome by assuming a bounded known function. In this section, an ANN [11] is utilized, where the unknown manipulation dynamics are approximated online.

First, an action NN is employed to approximate this unknown system dynamics. According to [12], a single-layer NN can be used to approximate any nonlinear continuous function over the compact set when the input layer weights are selected at random and held constant, whereas the output-layer weights are only tuned, provided that a sufficiently large number of nodes in the hidden layer are chosen. Therefore, a single-layer NN is employed here, whose output is defined as $\hat{w}_1^T \varphi(v_1^T X)$, where $\hat{w}_1 \in R^{n_1}$ and $v_1 \in R^{2 \times n_1}$ are the output and input layer weights, n_1 is the number of hidden-layer nodes, $\varphi(\cdot)$ is the activation function vector, and $X = [Y_p, D_2]^T \in R^2$ is

the action NN input. For simplicity, the action NN output is expressed as

$$\hat{F}(X) = \hat{w}_1^T \varphi(X). \tag{41}$$

Thus, ANN control input can be selected as

$$v = -\hat{F}(X) - \Lambda \dot{D}_2 - k_v r \tag{42}$$

where $k_v \in R$ is the feedback gain selected to be positive constant.

Applying (42) in (26) yields

$$\dot{r} = -k_v r + \left(F(X) - \hat{F}(X)\right) \tag{43}$$

$$\dot{r} = -k_v r + \tilde{F}(X) \tag{44}$$

where $\tilde{F}(X) = F(X) - \hat{F}(X)$ is the function approximation error. When the NN is properly trained and $\hat{F}(X)$ is an accurate estimate of $F(X)$, then $\tilde{F}(X) \to 0$, and (44) becomes

$$\dot{r} = -k_v r. \tag{45}$$

If k_v is properly selected as a positive constant, then, from (20) and (45), one can see that $e \to 0$, with $t \to \infty$. Thus, $D_2 = D_0$, and the sphere is said to be manipulated (pickup task), with D_1 continuously increasing.

The unknown function $F(X)$ can be approximated by the action NN as

$$F(X) = w_1^T \varphi\left(v_1^T X\right) + \varepsilon(X) = w_1^T \varphi(X) + \varepsilon(X) \tag{46}$$

where $w_1 \in R^{n_1}$ is the target output-layer weight, and $\varepsilon(X)$ is the NN approximation error. Define the weight estimation error $\tilde{w}_1 \in R^{n_1}$ by

$$\tilde{w}_1 = w_1 - \hat{w}_1. \tag{47}$$

Thus, (43) becomes

$$\dot{r} = -k_v r + \tilde{w}_1^T \varphi(X) + \varepsilon(X). \tag{48}$$

At the same time, a critic NN is implemented to evaluate the system performance index and tunes the action-generating NN. The input to the critic NN is chosen as [11]

$$z(t) = \int_0^t r^2(\tau) d\tau. \tag{49}$$

A choice of the critic NN signal is given by

$$R(t) = \hat{w}_2^T \sigma\left(v_2^T z(t)\right) = \hat{w}_2^T \sigma\left(z(t)\right) \tag{50}$$

where $\hat{w}_2 \in R^{n_2}$ and $v_2 \in R^{n_2}$ are the output- and input-layer weights, n_2 is the number of hidden-layer nodes, $\sigma(\cdot)$ is the hidden-layer activation function vector, and $z(t) \in R$ is the input to the NN. The critic NN input defines the long-term system performance over time. The critic signal $R(t)$ provides an additional corrective action based on the current and past performance. This information, along with filtered tracking error, is used to tune the action NN. The critic signal can also be viewed as a look ahead factor, which is determined based on the past performance. The proposed RLNN controller structure is depicted in Fig. 5. An inner-action-generating NN loop eliminates the nonlinear dynamics of the system, while the ANN critic design is modular, so that an existing industrial controller can be easily updated to obtain the proposed one by simply adding the inner NNs. This modular design avoids the need for the redesign of the industrial control systems [15].

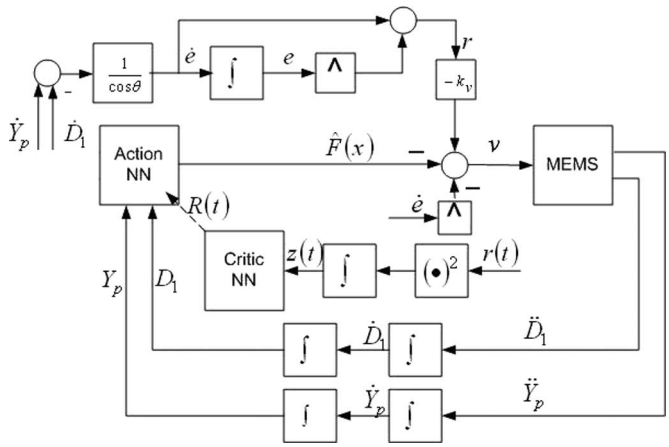

Fig. 5. NN controller architecture.

The next step is to determine the weight updates, so that the performance of the closed-loop tracking error dynamics is guaranteed.

Assumption 2: The desired trajectory D_0 is bounded, so that $|D_0| < D_B$, with D_B being a known scalar bound. In fact, D_0 becomes the interatomic distance.

Assumption 3: The NN approximation error $\varepsilon(X)$ is bounded above by $|\varepsilon(X)| < \varepsilon_N$ over the compact set.

Assumption 4: Both the ideal weights and the activation functions for all NNs are bounded by known positive values, so that

$$\|w_1\| \le w_{1\max} \quad \|w_2\| \le w_{2\max} \tag{51}$$

$$\|\sigma(\cdot)\| \le \sigma_{\max} \quad \|\varphi(\cdot)\| \le \varphi_{\max}. \tag{52}$$

Theorem 2: Consider the system given in (8)–(10), and take Assumptions 2–4. Let the action NN weight tuning algorithm be given by

$$\dot{\hat{w}}_1 = \varphi(X)\left(r - \hat{w}_1^T \varphi(X) + k_1 R(t)\right) \tag{53}$$

where k_1 is a design parameter, and $R(t)$ is the critic signal, which is given by the critic NN in (50). Let the critic NN weights be tuned by

$$\dot{\hat{w}}_2 = -\sigma\left(z(t)\right)\left(r + R(t)\right) \tag{54}$$

with the control signal selected by (42). Then, the filtered tracking error r and the NN weight estimates $\hat{w}_1$ and $\hat{w}_2$ are UUB, provided that

$$(1) \quad k_v > \frac{1}{2} \tag{55}$$

$$(2) \quad 0 < k_1 < 1. \tag{56}$$

Proof: Since $\dot{\tilde{w}}_1 = -\dot{\hat{w}}_1$, the updating rules (53) can be rewritten as

$$\begin{aligned}\dot{\tilde{w}}_1 &= \varphi(X)\left(-r + \hat{w}_1^T\varphi(X) - k_1 R(t)\right)\\ &= \varphi(X)\left(-r - \bar{e}_1 + w_1^T\varphi(X)\right.\\ &\qquad \left. + k_1\tilde{w}_2^T\sigma\left(z(t)\right) - k_1 w_2^T\sigma\left(z(t)\right)\right)\\ &= \varphi(X)\left(-r - \bar{e}_1 + k_1\bar{e}_2 + \eta_1 - k_1\eta_2\right) \qquad (57)\end{aligned}$$

where

$$\begin{aligned}\bar{e}_1 &= \tilde{w}_1^T\varphi(X)\\ \bar{e}_2 &= \tilde{w}_2^T\sigma\left(z(t)\right)\\ \eta_1 &= w_1^T\varphi(X)\\ \eta_2 &= w_2^T\sigma\left(z(t)\right). \qquad (58)\end{aligned}$$

Similarly, (54) can be rewritten as

$$\dot{\tilde{w}}_2 = \sigma\left(z(t)\right)\left(r - \bar{e}_2 + \eta_2\right). \qquad (59)$$

The Lyapunov function candidate is defined as

$$V = \frac{1}{2}\left(r^2 + \tilde{w}_1^T\tilde{w}_1 + \tilde{w}_2^T\tilde{w}_2\right). \qquad (60)$$

Differentiating (60) yields

$$\dot{V} = r\dot{r} + \tilde{w}_1^T\dot{\tilde{w}}_1 + \tilde{w}_2^T\dot{\tilde{w}}_2. \qquad (61)$$

Substitution of (48), (57), and (59) into (61) yields

$$\begin{aligned}\dot{V} &= r\left(-k_v r + \tilde{w}_1^T\varphi(X) + \varepsilon(X)\right)\\ &\quad + \tilde{w}_1^T\varphi(X)(-r - \bar{e}_1 + k_1\bar{e}_2 + \eta_1 - k_1\eta_2)\\ &\quad + \tilde{w}_2^T\sigma\left(z(t)\right)\left(r - \bar{e}_2 + \eta_2\right)\\ &\le \left(-k_v r^2 + r\varepsilon(X) + \frac{1}{2}\left(r^2 + \bar{e}_2^2\right)\right) + \left(-\bar{e}_2^2 + \bar{e}_2\eta_2\right)\\ &\quad + \left(-\bar{e}_1^2 + \frac{1}{2}k_1\left(\bar{e}_1^2 + \bar{e}_2^2\right) + \bar{e}_1\left(\eta_1 - k_1\eta_2\right)\right). \qquad (62)\end{aligned}$$

Simplify (62) to obtain

$$\begin{aligned}\dot{V} \le &-\frac{1}{2}(2k_v - 1)r^2 + r\varepsilon(X) - \frac{1}{2}(2 - k_1)\bar{e}_1^2\\ &+ \bar{e}_1(\eta_1 - k_1\eta_2) - \frac{1}{2}\left(1 - k_1\right)\bar{e}_2^2 + \bar{e}_2\eta_2. \qquad (63)\end{aligned}$$

Complete the square to obtain

$$\begin{aligned}\dot{V} \le &-\frac{1}{2}(2k_v - 1)\left(r - \frac{\varepsilon(X)}{(2k_v - 1)}\right)^2\\ &-\frac{1}{2}(2 - k_1)\left(\bar{e}_1 - \frac{(\eta_1 - k_1\eta_2)}{(2 - k_1)}\right)^2\\ &-\frac{1}{2}(1 - k_1)\left(\bar{e}_2 - \frac{\eta_2}{(1 - k_1)}\right)^2 + D^2 \qquad (64)\end{aligned}$$

where

$$D^2 \le D_{\max}^2 = \frac{1}{2}\left(\frac{\varepsilon_N^2}{(2k_v - 1)} + \frac{2\left(w_{1\max}^2\varphi_{\max}^2 + w_{2\max}^2\sigma_{\max}^2\right)}{2 - k_1} + \frac{w_{2\max}^2\sigma_{\max}^2}{1 - k_1}\right). \qquad (65)$$

This further implies that $\dot{V} < 0$ as long as (55) and (56) hold and

$$|r| > \frac{\varepsilon_N}{(2k_V - 1)} + \frac{\sqrt{2}D_{\max}}{\sqrt{2k_v - 1}} \qquad (66)$$

$$|\bar{e}_1| > \frac{w_{1\max}\varphi_{\max} + k_1 w_{2\max}\sigma_{\max}}{(2 - k_1)} + \frac{\sqrt{2}D_{\max}}{\sqrt{2 - k_1}} \qquad (67)$$

$$|\bar{e}_2| > \frac{w_{2\max}\sigma_{\max}}{(1 - k_1)} + \frac{\sqrt{2}D_{\max}}{\sqrt{1 - k_1}}. \qquad (68)$$

According to a standard Lyapunov extension theorem [7], this demonstrates that the filtered tracking error and the error in weight estimates are UUB. The boundedness of $|\bar{e}_1|$ and $|\bar{e}_2|$ implies that $\|\tilde{w}_1\|$ and $\|\tilde{w}_2\|$ are bounded, and this further implies that the weight estimates $\hat{w}_1$ and $\hat{w}_2$ are bounded.

D. ANN Controller With High-Gain Observer

In the preceding sections, the robust and adaptive NN controllers are proposed based on state feedback. However, in practical applications, Y_p and D_1 are usually observed by a laser measuring system [32] or a SEM [13], which has measurement noise, making the measurements inaccurate. In this regard, we extend our ANN controller to an output feedback version by implementing a high-gain observer. Similar extensions can be done for the robust controller.

Considering the system dynamics stated in (8)–(10), the separation principle can be applied to separate the state feedback controller scheme with the high-gain observer design [33].

By assuming that the outputs are y_1 and y_2, corresponding to Y_p and D_1, respectively, but with measurement noise, a high-gain observer is designated as

$$\begin{aligned}\dot{x}_1 &= x_2 + (2/\varepsilon_1)(y_1 - x_1)\\ \dot{x}_2 &= -F_{\rm bp}^{\rm VdW}/m_b + v/m_p + \left(1/\varepsilon_1^2\right)(y_1 - x_1)\\ y_1 &= Y_p + \rho_1\\ \dot{x}_3 &= x_4 + (2/\varepsilon_2)(y_2 - x_3)\\ \dot{x}_4 &= \left(F_{\rm bp}^{\rm VdW} - F_{\rm bs}^{\rm VdW}\right)/m_b + \left(1/\varepsilon_2^2\right)(y_2 - x_3)\\ y_2 &= D_1 + \rho_2 \qquad (69)\end{aligned}$$

where x_1 and x_2 are the estimates of Y_p and its velocity, whereas x_3 and x_4 are the estimates of D_1 and its velocity with ε_1, ε_2 are small design constants. Here, we introduce ρ_1 and ρ_2 as the measurement noise. Furthermore, the terms of $-F_{\rm bp}^{\rm VdW}/m_b$ and $(F_{\rm bp}^{\rm VdW} - F_{\rm bs}^{\rm VdW})/m_b$ in the second and fifth equations are the nominal model of the observer, which is a simplified version of the model discussed in the preceding

section, considering the fact that van der Waals forces are the dominant adhesive forces [1] and $m_p \gg m_b$.

Assumption 5: The measurement noise and their derivatives up to the second order are bounded [34] by $|\rho_i| \leq \rho_{iN}$, $|\dot{\rho}_i| \leq \rho'_{iN}$, and $|\ddot{\rho}_i| \leq \rho''_{iN}$ for $i = 1, 2$.

Assumption 6: The derivatives of functions $F_1(Y_p)$ and $F_2(D_1)$ over the compact set are bounded by $|\dot{F}_1| \leq F'_{1M}$ and $|\dot{F}_2| \leq F'_{2M}$.

Assumption 6 is a mild assumption from microscale physics, implying that there will be no change in the force by infinite magnitude.

By applying the separation principle, an output feedback ANN controller is obtained by replacing the states Y_p and D_1 by their estimates x_1 and x_3, which were provided by the high-gain observer in (69), respectively. In other words, the control input is now selected as

$$v = -\hat{F}(\hat{X}) - \Lambda \dot{\hat{D}}_2 - k_v \hat{r} \tag{70}$$

where $\hat{X} = [x_1, \hat{D}_2]^T \in R^2$, $\hat{D}_2 = x_1 - x_3 - 2R_b$, $\dot{\hat{D}}_2 = x_2 - x_4$, and $\hat{r} = \dot{\hat{D}}_2 + \Lambda(\hat{D}_2 - D_0)$. The updating laws for NNs are also changed to

$$\dot{\hat{w}}_1 = \varphi(\hat{X}) \left(\hat{r} - \hat{w}_1^T \varphi(\hat{X}) + k_1 \hat{R}(t) \right) \tag{71}$$

$$\dot{\hat{w}}_2 = -\sigma\left(\hat{z}(t)\right) \left(\hat{r} + \hat{R}(t) \right) \tag{72}$$

where $\hat{R}(t) = \hat{w}_2^T \sigma(\hat{z}(t))$, and $\hat{z}(t) = \int_0^t \hat{r}^2(\tau) d\tau$.

Hence, we have following theorem.

Theorem 3: Consider the system given in (8)–(10) and the output feedback controller (70) with updating laws (71) and (72). Let Assumptions 5 and 6 hold. Considering the original state feedback controller (42) and the updating laws (53) and (54), the filtered tracking error and the NN weight estimates are UUB. Then, there exists ε_{1M} and ε_{2M}, such that, for every $0 < \varepsilon_1 < \varepsilon_{1M}$ and $0 < \varepsilon_2 < \varepsilon_{2M}$, the filtered tracking error and the NN weight estimates of the closed-loop system with the output feedback controller (70) are UUB.

Proof: The proof is divided into two steps. The first step is to take care of the measurement noise. The second step is to prove the UUB of the closed-loop system.

In the first step, consider the observer for D_1. Let $z_1 = Y_p + \rho_1$ and $z_2 = \dot{Y}_p + \dot{\rho}_1$. The original system (9) and the output can be rewritten as

$$\begin{aligned} \dot{z}_1 &= z_2 \\ \dot{z}_2 &= F_1(z_1 - \rho_1) + v + \ddot{\rho}_1 \\ y_1 &= z_1. \end{aligned} \tag{73}$$

Furthermore, by using the mean value theorem, one can rewrite (73) as

$$\begin{aligned} \dot{z}_1 &= z_2 \\ \dot{z}_2 &= F_1(z_1) + v - \dot{F}_1(\zeta_1)\rho_1 + \ddot{\rho}_1 \\ y_1 &= z_1 \end{aligned} \tag{74}$$

where $\zeta_1 \in [0 \quad \rho_1]$, or $\zeta_1 \in [\rho_1 \quad 10]$. Thus, $-\dot{F}_1(\zeta_1)\rho_1 + \ddot{\rho}_1$ can be considered as a disturbance, which appears from Assumptions 5 and 6 to be bounded. In other words, a new reference system without measurement noise can be constructed. The same analysis applies for D_1. Such a high-gain-observer-design-based system is thoroughly discussed in [33]. Moreover, one can readily assert that the ANN controller based on state feedback can be translated to system (74) with UUB stability.

Thereafter, the second step is similar to the proof in [33] and thus omitted in this paper. As a result, the tracking error in terms of z_1, z_2, and the NN weight estimates is UUB. Due to the boundedness of the measurement noise, one can conclude that the filtered tracking error and the NN weight estimates of the original closed-loop system are UUB.

VI. Simulation Result

To substantiate our methods, simulation results are shown in this section. The purpose of the controller is to provide a control force for the probe to pick up the microobject. Initially, it is assumed that the object is in contact with the substrate before it is picked up by the probe. The controller provides the force to cause the actual capture and to retain the microsphere at the tip of the probe. Once the capture occurs, and the external force to be applied through the probe is determined and maintained to keep the microsphere attached to the probe.

The dynamics of the system is expressed as (8)–(10), where $m_p = 1.0 \times 10^{-5}$ kg is the mass of the probe, $m_b = 1.0 \times 10^{-7}$ kg is the mass of the microsphere, and $R_b = 50$ μm is the radius of the microsphere. Initially, the probe is assumed to park right above the object at a height of 100 μm, which means that the approaching angle $\theta = 0^\circ$. That is also the typical way to approach microobjects for capturing [4], [26]. The surface roughness is assumed to be 1.0×10^{-10} m [27]. The humidity is arbitrarily set to 50% [28]. To testify the controller designs, model uncertainties and environmental noise are added in the systems (8) and (9) in Gaussian form with zero mean and $\sigma^2 = 1.0 \times 10^{-9}$ N^2.

For comparison, a traditional proportional–differential (PD) controller is first designed based on the filtered tracking error with the control input selected as $v = -\Lambda \dot{D}_2 - k_v r$, where $k_v = 5$ and $\Lambda = 10^{-3}$. Fig. 6 shows the trajectories of the probe and microobject, whereas Fig. 7 shows the control input. In Fig. 6, the trajectories of D_1 and $D_2 - D_0$ are depicted. The goal of the controller is to drive the probe to adhere the particle, which means that D_1 should increase while maintaining $D_2 - D_0$ to be zero at the same time in order to keep the object in tact. Although the PD controller is easy to implement and capable of picking up the microsphere, it was found that the applied force appears to be highly oscillatory, as depicted in Fig. 7. These oscillations might damage the fragile sample or even the probe.

By contrast, Fig. 8 displays the trajectories, and Fig. 9 depicts the applied force on the probe by using a robust controller. The controller parameters are also chosen as $k_v = 5$ and $\Lambda = 10^{-3}$ in (27). In estimating $F(X)$, we set $\hat{F}(X) = 1/m_b(F_{\rm bs}^{\rm VdW} - F_{\rm bp}^{\rm VdW}) = A_{\rm bs}^w R_b / 6 m_b (1/D_1 - 1/6D_2)$ since, usually, van der Waals force is the dominant adhesive force [1] and $m_p \gg m_b$. Furthermore, $F_M(X) = \hat{F}(X)/10$, and $\beta = 0.1$ μm in (36).

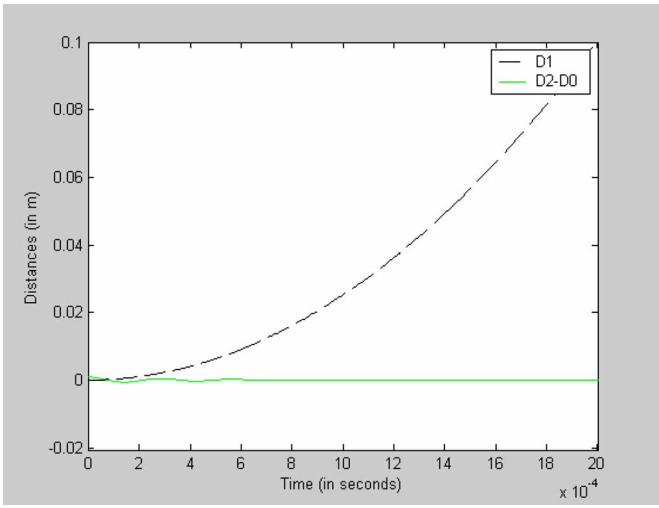

Fig. 6. Displacement using a conventional PD controller. The trajectory of D_2-D_0 denotes the distance between the probe and the microparticle (solid line). The trajectory of D_1 represents the distance between the substrate and the particle (dashed line).

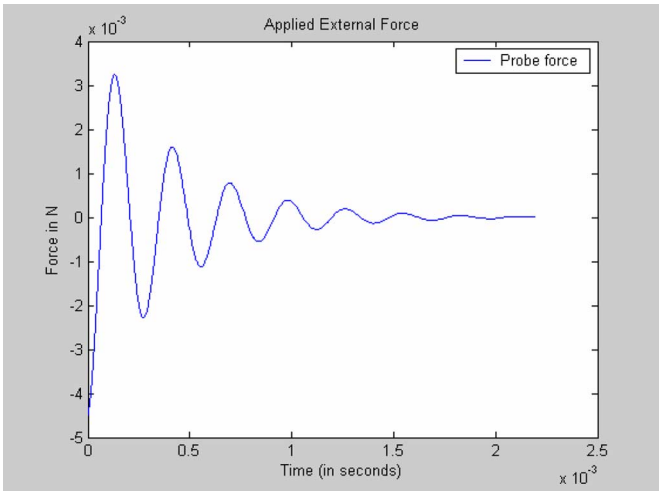

Fig. 7. Applied external force using a conventional PD controller.

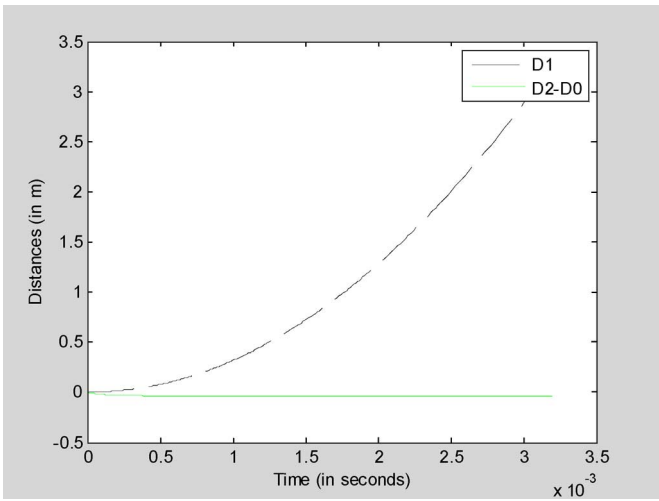

Fig. 8. Displacement using a robust controller. The trajectory of D_2-D_0 denotes the distance between the probe and the microparticle (solid line). The trajectory of D_1 represents the distance between the substrate and the particle (dashed line).

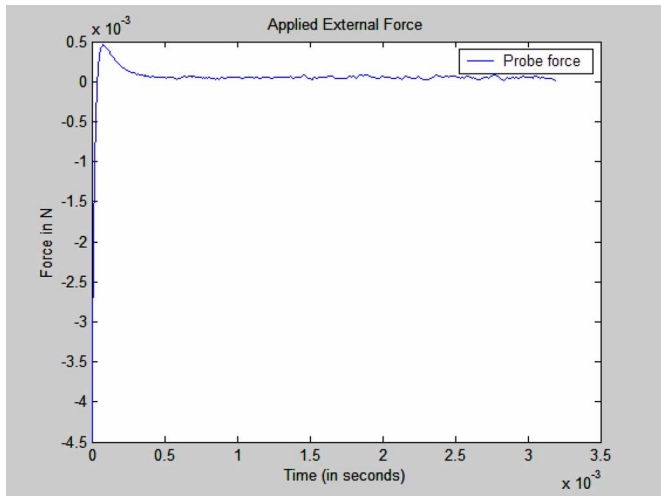

Fig. 9. Applied external force using a robust controller.

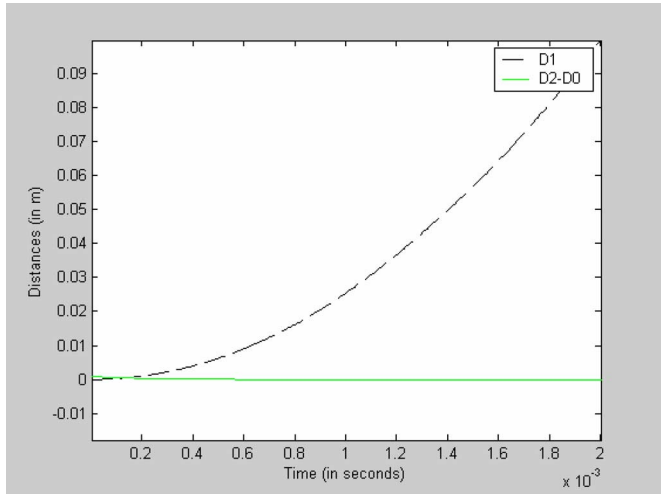

Fig. 10. Displacement using with an adaptive critic NN controller. The trajectory of D_2-D_0 denotes the distance between the probe and the microparticle (solid line). The trajectory of D_1 represents the distance between the substrate and the particle (dashed line).

The results show that the robust controller could avoid the large-scale force oscillation before grabbing the object successfully. However, due to the model uncertainties and other unknown parameters, the controller output still demonstrates a small fluctuation.

Fig. 10 shows the distances, whereas Fig. 11 shows the control input resulting from using a reinforcement-learning-based controller with $k_v = 5$, $\Lambda = 10^{-3}$, and $k_1 = 0.8$. In both the action and critic NNs, the hyperbolic tangent sigmoid transfer function is used. The hidden layer of the action NN consists of ten nodes, while the critic NN consists of five nodes. The simulation results show that the NN controller can approximate the unknown system dynamics and avoid the oscillation phenomenon. Furthermore, because of the learning ability of NN, the influence of the unknown uncertainties is greatly reduced.

For quantifying the comparison results, we utilize a cost function to measure the performance of each controller, which

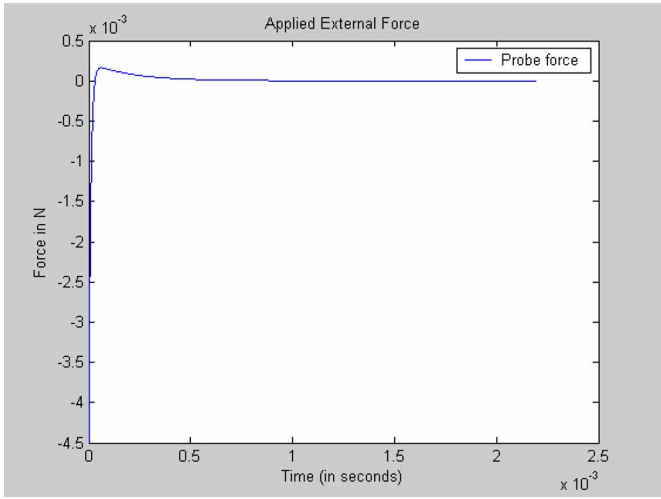

Fig. 11. Applied external force with an adaptive critic NN controller.

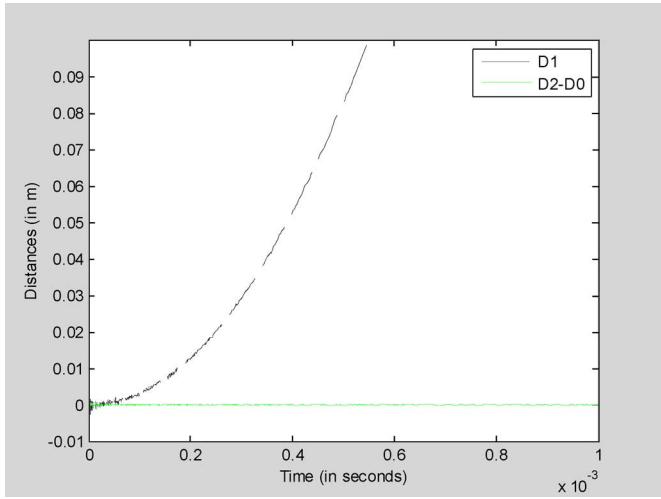

Fig. 12. Displacement using with an output feedback adaptive critic NN controller. The actual trajectory of D_2-D_0 denotes the distance between the probe and the microparticle (solid line). The actual trajectory of D_1 represents the distance between the substrate and the particle (dashed line).

TABLE I
PERFORMANCE COMPARISON

Controller type	$J(t_0,t_f)$
PD controller	539.45
Robust controller	231.63
NN controller	168.75

is widely used for comparing control designs [17], [18]. In this paper, we define a standard quadratic cost function as

$$J(t_0,t_f)=\int_{t_0}^{t_f}\left(D_2(t)-D_0\right)^T Q\left(D_2(t)-D_0\right)+v^T(t)Rv(t)dt \tag{75}$$

where R and Q are positive definite matrices (they are scalar in our case). t_0 is the initial time, while t_f is the final time of the simulation. One can see that (75) represents the amount of effort that the controller needs, which becomes a measure of the system response. In this paper, the parameters are set to $Q=10^4$, $R=10^6$, $t_0=0$ ms, and $t_f=3.2$ ms, respectively. As a result, the performance index for each controller is shown in Table I.

Mainly due to the additional robust auxiliary input, the robust controller design is able to produce a more stable control signal while achieving a much better outcome than the PD design in terms of cost. From the table, we can find that the PD controller requires more than double the effort than others. Moreover, since a critic NN is introduced to evaluate the system performance, the ANN controller succeeds in obtaining the best cost.

Moreover, to testify the feasibility of our output feedback ANN controller, the simulation is carried on with parameters $\varepsilon_1=\varepsilon_2=0.01$ in (69). The measurement noise is also added in the simulation as dual-tone form [34] $\rho_{1,2}=(\sin(t)+0.5\sin(3.33t))\times 10^{-6}$ m for both D_1 and Y_p. The system response and the actual applied force are plotted in Figs. 12 and 13. Although there appears to be a huge variation of control input at the beginning due to the measurement noise and

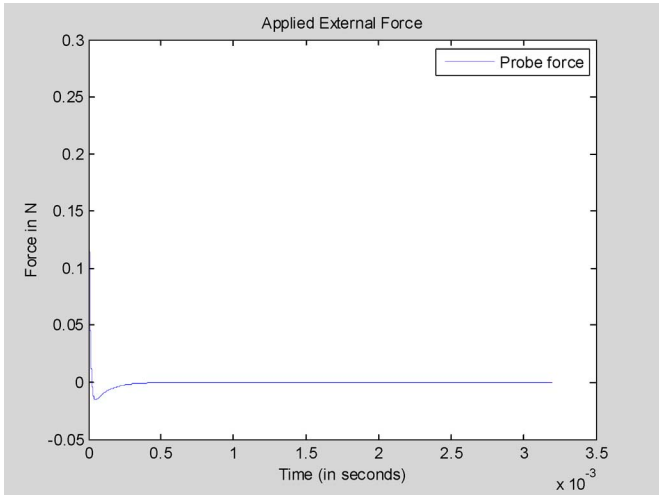

Fig. 13. Applied external force using an output feedback adaptive critic NN controller.

observer convergence issues, the control input soon becomes steady, indicating that the observer approximates the actual states.

Meanwhile, for the convenience of comparison, the displacement of D_1 and D_2-D_0 for all the controllers is demonstrated in Figs. 14 and 15, respectively using the same scale. It can be seen that capture occurs around 10^{-3} s for the proposed robust and the robust NN controllers (both state feedback and output feedback) since the applied force and trajectory D_2-D_0 stabilizes. By contrast, it takes a bit longer to capture the microsphere by using the PD controller.

VII. CONCLUSION

In this paper, a suite of robust manipulation controllers was presented for the pickup task of a microsphere. Closed-loop stability is demonstrated using a robust controller by assuming that the upper bound on the unknown dynamics of the contact forces is known. Then, a reinforcement-learning-based adaptive

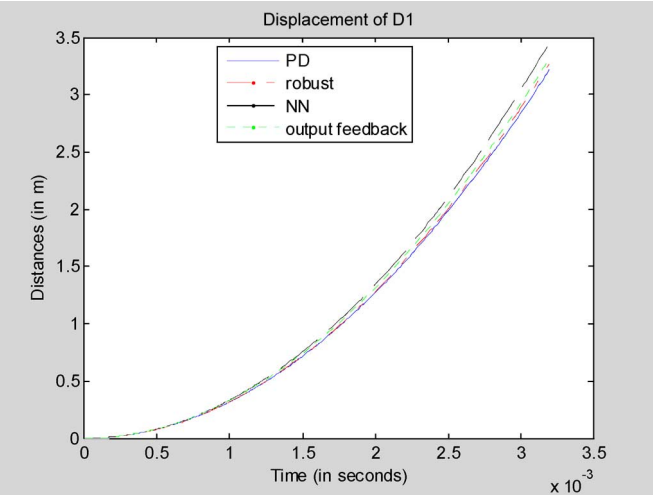

Fig. 14. Displacement of D_1 for all controller designs.

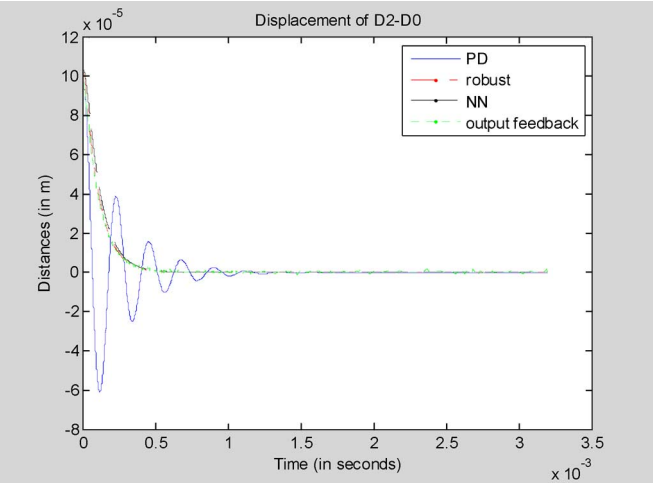

Fig. 15. Displacement of $D_2 - D_0$ for all controller designs.

NN controller was presented for the task of picking up a microsphere from a substrate, wherein the need to know an upper bound on the unknown dynamics is relaxed. The controllers have been proven to have guaranteed stability, whereas the task of manipulation was possible even when the nonlinearities and uncertainties are not modeled for. Simulation results indicate that the robust controller and the NN controller outperform a conventional PD controller in terms of the response time and applied force during the object manipulation. Furthermore, the NN controller has an advantage over the robust controller with regard to tolerating model uncertainties and noise. The comparison is strengthened by using a standard quadratic cost function. To mitigate the lack of feedback of certain states and the presence of measurement noise, an output feedback adaptive critic-based NN controller with high-gain observer is proposed and verified in a simulation environment.

As part of future work, experiments need be carried out to substantiate our theoretical conclusions. A better model should be built based on experimental data. Additionally, a more satisfactory estimate of $F(X)$ has to be selected for robust control.

ACKNOWLEDGMENT

The authors would like to thank the anonymous reviewers for their helpful comments and P. He and V. Janardhan for initiating this research topic and for their contributions.

REFERENCES

[1] J. T. Feddema, P. Xavier, and R. Brown, "Micro-assembly planning with van der Waals force," in *Proc. IEEE Int. Symp. Assembly Task Planning*, 1999, pp. 32–38.

[2] F. Arai, D. Andou, and T. Fukuda, "Adhesion forces reduction for micro manipulation based on micro physics," in *Proc. MEMS, 9th Annu. Int. Workshop Investigation Micro Struct., Sens., Actuators, Mach. Syst.*, Feb. 11–15, 1996, pp. 354–359.

[3] M. Sitti, "Survey of nanomanipulation systems," in *Proc. IEEE-Nanotechnology Conf.*, Maui, HI, Nov. 2001, pp. 75–80.

[4] Y. Rollot, S. Regnier, S. Haliyo, L. Buchaillot, J. C. Guinot, and P. Bidaud, "Experiments on micromanipulation using adhesion forces in unconstrained environment," in *Proc. IEEE/RS Int. Conf. Intell. Robots Syst.*, 2000, vol. 1, pp. 653–658.

[5] F. Arai, D. Andou, Y. Nonoda, T. Fukuda, H. Iwata, and K. Itoigawa, "Integrated microendeffector for micromanipulation," *IEEE/ASME Trans. Mechatronics*, vol. 3, no. 1, pp. 17–23, Mar. 1998.

[6] S. Saito, H. Miyazaki, and T. Sato, "Pick and place operation of a microobject with high reliability and precision based on micro-physics under SEM," in *Proc. IEEE Int. Conf. Robot. Autom.*, 1999, vol. 4, pp. 2736–2743.

[7] F. L. Lewis, S. Jagannathan, and A. Yesilderik, *Neural Network Control of Robot Manipulators and Nonlinear Systems*. New York: Taylor & Francis, 1999.

[8] P. J. Werbos, "Neurocontrol and supervised learning: An overview and evaluation," in *Handbook of Intelligent Control*, D. A. White and D. A. Sofge, Eds. New York: Van Nostrand Reinhold, 1992, pp. 65–90.

[9] A. G. Barto, "Reinforcement learning and adaptive critic methods," in *Handbook of Intelligent Control*, D. A. White and D. A. Sofge, Eds. New York: Van Nostrand Reinhold, 1992, pp. 469–492.

[10] B. Igelnik and Y. H. Pao, "Stochastic choice of basis functions in adaptive function approximation and the functional-link net," *IEEE Trans. Neural Netw.*, vol. 6, no. 6, pp. 1320–1329, Nov. 1995.

[11] V. Janardhan, P. He, and S. Jagannathan, "Neural network controller for the manipulation of microscale objects," in *Proc. IEEE Symp. Intell. Control*, 2004, pp. 55–60.

[12] M. P. Boukallel and J. Abadie, "Micromanipulation tasks using passive levitated force sensing manipulator," in *Proc. IEEE/RSJ Int. Conf. IROS*, Oct. 2003, pp. 529–534.

[13] K. Koyano and T. Sato, "Micro object handling system with concentrated visual fields and new handling skills," in *Proc. IEEE Conf. Robot. Autom.*, 1996, pp. 2541–2548.

[14] H. Miyazaki and T. Sato, "Pick and place shape forming of three-dimensional micro structures from fine particles," in *Proc. IEEE Int. Conf. Robot. Autom.*, Apr. 1996, pp. 2535–2540.

[15] S. Jagannathan and G. Galan, "Adaptive critic neural network-based object grasping control using a three-finger gripper," *IEEE Trans. Neural Netw.*, vol. 15, no. 2, pp. 395–407, Mar. 2004.

[16] P. J. Werbos, "New directions in ACDS: Keys to intelligent control and understanding the brain," in *Proc. IEEE-INNS-ENNS Int. Joint Conf. Neural Netw.*, 2000, vol. 3, pp. 61–66.

[17] D. Prokhrov and D. C. Wunch, "Adaptive critic designs," *IEEE Trans. Neural Netw.*, vol. 8, no. 5, pp. 997–1007, Sep. 1997.

[18] D. Han and S. N. Balakrishnan, "State-constrained agile missile control with adaptive-critic-based neural networks," *IEEE Trans. Control Syst. Technol.*, vol. 10, no. 4, pp. 481–489, Jul. 2000.

[19] J. Israelachvili, "The nature of van der Waals forces," *Contemp. Phys.*, vol. 15, no. 2, pp. 159–177, 1974.

[20] P. A. Thompson and M. O. Robbins, "Simulations of contact-line motion: Slip and the dynamic contact angle," *Phys. Rev. Lett.*, vol. 63, no. 7, pp. 766–769, Aug. 1989.

[21] J. Crassous, E. Charlaix, H. Gayvallet, and J. Loubert, "Experimental study of a nanometric liquid bridge with a surface force apparatus," *Langmuir*, vol. 9, no. 8, pp. 1995–1998, 1993.

[22] S. Jagannathan and Q. Yang, "A robust controller for the manipulation of micro-scale objects," in *Proc. ACC*, 2005, pp. 4154–4159.

[23] F. Ohkawa and Y. Yonegawa, "A discrete model reference adaptive control system for a plant with input amplitude constraints," *Int. J. Control*, vol. 36, no. 5, pp. 747–753, 1982.

[24] S. P. Karason and A. M. Annaswamy, "Adaptive control in the presence of input constraints," *IEEE Trans. Autom. Control*, vol. 39, no. 11, pp. 2325–2330, Nov. 1994.
[25] F. Z. Chaoui, F. Giri, J. M. Dion, M. M-Saad, and L. Dugard, "Direct adaptive control subject to input amplitude constraint," *IEEE Trans. Autom. Control*, vol. 45, no. 3, pp. 485–490, Mar. 2000.
[26] H. Miyazaki and T. Sato, "Pick and place shape forming of three-dimensional micro structures from fine particles," in *Proc. IEEE ICRA*, 1996, pp. 2535–2540.
[27] Q. Zhou, P. Kallio, F. Arai, T. Fukuda, and H. Koivo, "A model for operating spherical micro objects," in *Proc. Int. Symp. MHS*, 1999, pp. 79–85.
[28] Y. Rollot, S. Regnier, and J. C. Guinot, "Dynamical model for the micromanipulation by adhesion: Experimental validations for determined conditions," *Int. J. Micromechatron.*, vol. 1, no. 4, pp. 273–297, 2002.
[29] M. Sitti and H. Hashimoto, "Tele-nanorobotics using atomic force microscope," in *Proc. IEEE/RSJ Int. Conf. IROS*, 1998, pp. 1739–1746.
[30] J. T. Feddema, P. Xavier, and R. Brown, "Assembly planning at the micro scale," in *Prof. IEEE Int. Conf. Robot. Autom.*, Leuven, Belgium, 1998, pp. 16–21.
[31] S. Saito, H. Himeno, and K. Takahashi, "Electrostatic detachment of an adhering particle from a micromanipulated probe," *J. Appl. Phys.*, vol. 93, no. 4, pp. 2219–2224, Feb. 2003.
[32] A. Buerkle and S. Fatikow, "Laser measuring system for a flexible microrobot-based micromanipulation station," in *Proc. IEEE/RSJ Int. Conf. IROS*, 2000, pp. 799–804.
[33] H. K. Khalil, *Nonlinear Systems*. Englewood Cliffs, NJ: Prentice-Hall, 2002.
[34] H. S. Sane, D. S. Bernstein, and H. J. Sussmann, "Lyapunov-based output-feedback adaptive stabilization of minimum phase second-order systems," in *Proc. IEEE Conf. Decision Control*, 2001, vol. 2, pp. 1181–1186.
[35] J. Israelachvili, *Intermolecular and Surface Forces*. New York: Academic, 1991.

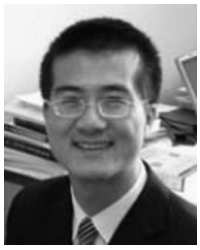

Qinmin Yang (S'05) was born in Hengyang, China, in 1979. He received the B.S. degree from the Civil Aviation University of China, Tianjin, in 2001, the M.S. degree from the Chinese Academy of Sciences, Beijing, in 2004, and the Ph.D. degree from the University of Missouri-Rolla, Rolla, in 2007, all in electrical engineering.

He is currently a Postdoctoral Research Associate with the Department of Electrical and Computer Engineering, University of Missouri-Rolla. His research interests include intelligent control, neural network learning, nanorobotics, autonomous systems/mobile robotics, and system diagnosis.

S. Jagannathan (M'95–SM'99) received the B.S. degree from Anna University, Madras, India, in 1987, the M.S. degree from the University of Saskatchewan, Saskatoon, SK, Canada, in 1989, and the Ph.D. degree from the University of Texas, Arlington, in 1994, all in electrical engineering.

From 1986 to 1987, he was a Junior Engineer with Engineers India Ltd., New Delhi. From 1990 to 1991, he was a Research Associate and an Instructor with the University of Manitoba, Winnipeg, MB, Canada. From 1994 to 1998, he was a Consultant with the Systems and Controls Research Division, Caterpillar Inc., Peoria, IL. From 1998 to 2001, he was with the University of Texas, San Antonio. Since September 2001, he has been with the Department of Electrical and Computer Engineering, University of Missouri-Rolla, where he is currently a Professor. He is also the Site Director for the National Science Foundation Industry (NSF)/University Cooperative Research Center on Intelligent Maintenance Systems. He is the coauthor of more than 180 refereed conference proceedings and juried journal articles; several book chapters; and three books entitled *Neural Network Control of Robot Manipulators and Nonlinear Systems* (Taylor & Francis, 1999), *Discrete-Time Neural Network Control of Nonlinear Discrete-Time Systems* (CRC Press, 2006), and *Wireless Ad Hoc and Sensor Networks: Performance, Protocols and Control* (CRC Press, 2007). He is the holder of 17 patents, with several that are still in process. His research interests include adaptive and neural network control, computer/communication/sensor networks, prognostics, and autonomous systems/robotics.

Dr. Jagannathan is a member of Tau Beta Pi, Eta Kappa Nu, and Sigma Xi and the IEEE Committee on Intelligent Control. He has served and currently serving on the program committees of several IEEE conferences. He is an Associate Editor for the IEEE TRANSACTIONS ON CONTROL SYSTEMS TECHNOLOGY, IEEE TRANSACTIONS ON NEURAL NETWORKS, IEEE TRANSACTIONS ON SYSTEMS ENGINEERING, and serves on several program committees. He is currently serving as the Program Chair for the 2007 IEEE International Symposium on Intelligent Control and the Publicity Chair for the 2007 International Symposium on Adaptive Dynamic Programming. He was the recipient of several gold medals and scholarships during his undergraduate program, the Region 5 IEEE Outstanding Branch Counselor Award in 2006, the Faculty Excellence Award in 2006, the St. Louis Outstanding Branch Counselor Award in 2005, the Teaching Excellence Award in 2005, the Caterpillar Research Excellence Award in 2001, the Presidential Award for Research Excellence at UTSA in 2001, the NSF CAREER award in 2000, the Faculty Research Award in 2000, the Patent Award in 1996, and the Sigma Xi "Doctoral Research Award," in 1994.